## Control of Effective Cooling Rate upon Magnetron Sputter Deposition of Glassy Ge<sub>15</sub>Te<sub>85</sub>

Julian Pries<sup>1</sup>, Shuai Wei<sup>1</sup>, Felix Hoff<sup>1</sup>, Pierre Lucas<sup>2\*</sup> Matthias Wuttig<sup>1,3</sup>

Keywords: Metastable phases, chalcogenide glasses, glass transition, fictive temperature, quenching, undercooling

Reducing the enthalpy of as-deposited amorphous films is desirable as it improves their kinetic stability and enhances the reliability of resulting devices. Here we demonstrate that  $Ge_{15}Te_{85}$  glass films of lower enthalpy are produced by increasing the voltage during magnetron sputter deposition. An increase of ~100 V leads to a drop in effective cooling rate of almost three orders of magnitude, thereby yielding markedly lower enthalpy glasses. The sputtering voltage therefore constitutes a novel parameter for tuning the fictive temperature of glass films, which could help to obtain ultra-stable glasses in combination with substrate temperature control.

The fabrication of amorphous films is essential for multiple technologies ranging from integrated optics to phase change material (PCM) memory devices. Glassy (amorphous) materials are intrinsically out of thermodynamic equilibrium and their physical properties tend to evolve over time as they relax towards a lower enthalpy state [1-3]. These unwanted changes can be mitigated by producing glasses with low initial enthalpy at slow cooling rates upon vitrification, or post processing by annealing. It was also recently shown that ultra-stable glasses (USGs) can be obtained by physical vapor deposition (PVD) on substrates heated near the glass transition temperature  $T_{\rm g}$  [4, 5]. This phenomenon was associated with the enhanced mobility of the constituent particles on the film surface, which provided sufficient flexibility to access the lowest minima in the energy landscape. Here we investigate the effect of increasing the kinetic energy of constituent particles during magnetron sputtering of glassy  $Ge_{15}Te_{85}$  films. The effective cooling rate of sputtered films is estimated by calorimetry. It is found that the final enthalpy and fictive temperature of glass films can be controlled by tuning the sputtering voltage.

While most glasses are prepared by fast cooling from the melt [6], glass films for device applications are frequently produced by PVD. In the case of PCMs, significant differences in physical properties between as-deposited and melt-quenched samples have been reported, including the atomic arrangement, the amorphous phase

<sup>&</sup>lt;sup>1</sup>Institute of Physics IA, RWTH Aachen University, 52074 Aachen, Germany

<sup>&</sup>lt;sup>2</sup>Department of Materials Science and Engineering, University of Arizona, Tucson, AZ, 85712, United States

<sup>&</sup>lt;sup>3</sup>Peter Grünberg Institute (PGI 10), Forschungszentrum Jülich, 52428 Jülich, Germany

<sup>\*</sup>Email adress: pierre@email.arizona.edu

stability and the crystal growth velocity [7-9]. Large differences in cooling rates and vitrification processes lead to density and enthalpy changes that could account for these property modifications [10]. Yet, while the cooling rate during melt-quenching may be known, the effective cooling rate of sputter-deposited films remains unknown, rendering a comparison infeasible. It is therefore of interest to derive an effective cooling rate for as-deposited glasses. Fortunately, the cooling rate of a glass can be derived from its fictive temperature  $T_{\rm f}$ , measured calorimetrically [11]. Prominent PCMs such as Ge<sub>2</sub>Sb<sub>2</sub>Te<sub>5</sub> or (Ag,In)-doped Sb<sub>2</sub>Te (AIST) [12] or bad glass formers. Hence, the measurement of the glass transition temperature  $T_{\rm g}$  is very challenging. On the contrary, Ge<sub>15</sub>Te<sub>85</sub> is a good model system for a comparative study of different glassy states as it is a good glass former that exhibits a complete calorimetric glass transition [13]. This enables an unambiguous determination of  $T_{\rm f}$ . It can be vitrified by cooling from the undercooled liquid (UCL) to produce glasses of known cooling rates and enthalpy for comparison with as-deposited samples (ASD). It is moreover relevant to PCMs, as it consists of the same elements as the PCM GeTe. Amorphous films of Ge<sub>15</sub>Te<sub>85</sub> were therefore produced by magnetron sputter deposition using a sputtering power of 6 to 120 W corresponding to a sputtering voltage ranging from 260 to 370 V, respectively. Melt-quenched (MQ) glasses were produced for comparison with ASD glasses by heating  $Ge_{15}Te_{85}$  up to well above its glass transition temperature  $T_g$  into the UCL phase and subsequently cooling at a constant rate  $\theta_c$  of 3, 6, 10, 20 and 40 K/min in a differential scanning calorimeter (DSC).

Since materials fall out of the metastable equilibrium of the UCL at different temperatures depending on  $\theta_c$ , the enthalpy states of the resulting glasses differ [14]. If the heat capacity of the UCL is approximated as a constant  $C_p^{\text{UCL}}(T) \approx const.$ , where T is temperature, the enthalpy of the UCL  $H^{\text{UCL}}(T)$  is a linear function in temperature. When the heat capacity of a glass  $C_p^{\text{g}}(T)$  is independent of cooling rate during vitrification and approximately a constant as a function of T as well, the difference in enthalpy between two glasses i and j is given by

$$\Delta H_{g,i}^{g,j} = \Delta C_{p} \cdot \left( T_{f,i} - T_{f,j} \right), \tag{1}$$

where  $\Delta C_{\rm p}$  is the heat capacity difference between  $C_{\rm p}^{\rm UCL}$  and  $C_{\rm p}^{\rm g}$ . With these approximations  $\Delta H_{{\rm g},i}^{{\rm g},j}$  is independent of temperature as long as structural relaxation is negligible. Utilizing the standard fictive temperature  $T_{\rm f}^{\rm s}$  of a glass formed at the standard cooling rate  $\theta_{\rm c}^{\rm s}$  of 20 K/min as a reference, the enthalpy difference between a glass and the standard glass becomes [14]

$$\Delta H_{\rm g}^{\rm s}(T_{\rm f}) = \Delta C_{\rm p} \cdot (T_{\rm f} - T_{\rm f}^{\rm s}) , \qquad (2)$$

which is a linear function of  $T_{\rm f}$  while all other parameters are material constants. Moreover, the fictive temperature near  $T_{\rm f}^{\rm s}$  depends on  $\theta_{\rm c}$  according to [11, 14]

$$T_{\rm f}(\theta_{\rm c}) = T_{\rm f}^{\rm s} \cdot \left(1 - \frac{1}{m} \cdot \log_{10} \left(\frac{\theta_{\rm c}}{\theta_{\rm c}^{\rm s}}\right)\right)^{-1},\tag{3}$$

where m is the fragility of the material which can be quantified by the slope in viscosity  $\eta$  at the standard glass transition temperature  $T_g^s = T_f^s$  at 20 K/min in the so-

called Angell-plot [6, 15]. Therefore,  $\Delta H_g^s$  is a linear function of  $T_f$  only, which itself is only a function of cooling rate  $\theta_c$ .

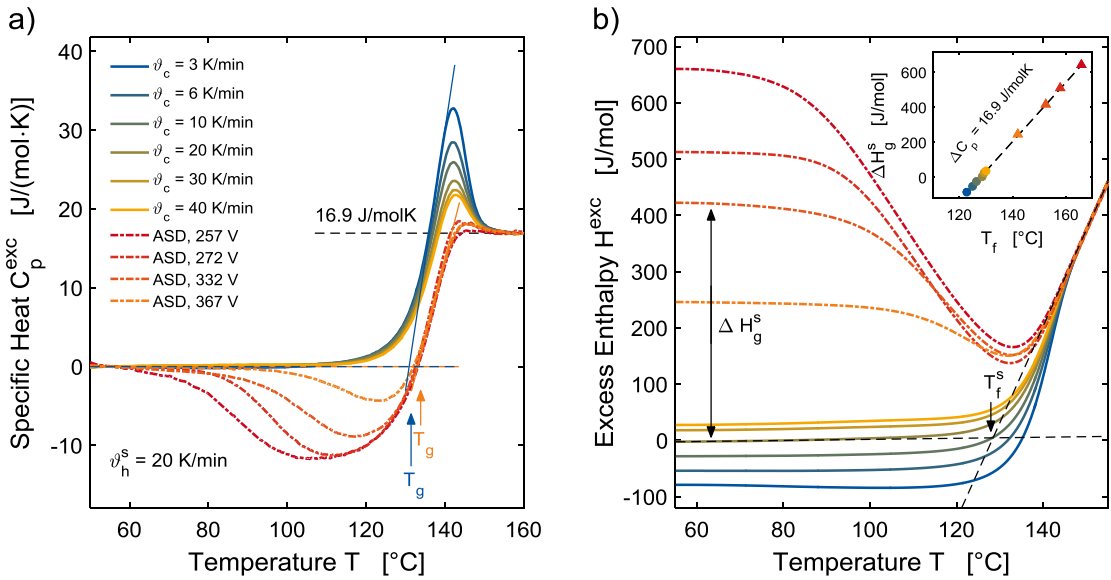


Figure 1: Calorimetric response of melt-quenched (MQ) and as-deposited (ASD)  $Ge_{15}Te_{85}$  glasses upon heating at the standard heating rate  $\theta_h^s = 20$  K/min.  $C_p^{\rm exc}(T)$  is the crystalline rescan-subtracted heat capacity measured in DSC. This excess heat capacity  $C_p^{\rm exc}(T)$  in **a**) for MQ glasses shows an increased endothermic overshoot upon glass transition when the cooling rate is lowered. The endothermic overshoot is almost suppressed for ASD glasses, which instead feature a pronounced exothermic heat release prior to glass transition. This exothermic heat release is usually indicative for glasses formed with a much higher cooling rate than the subsequent heating rate. Accordingly, the exothermic heat release is absent in the slowly cooled MQ glasses. Since both, amorphous MQ and ASD  $Ge_{15}Te_{85}$  show a glass transition, they have to be in the glassy state at lower temperatures. All glasses show a difference in heat capacity between the glassy and the UCL state of about 16.9 J/molK (0.175 meV/atomK). **b**) From the integrated  $C_p^{\rm exc}(T)$  curves normalized in the UCL, the enthalpy difference between glassy states becomes apparent on the low temperature side. The enthalpy difference  $\Delta H_g^s$  is much smaller for MQ glasses than for ASD ones, indicating that ASD glasses are less stable in this case. The fictive temperature is found at the crossing point of the extrapolated enthalpy of the glassy and UCL phase, as indicated by the arrow in b) for the standard glass.

In order to derive the effective cooling rate of ASD sputtered films, we first show that Eq.(2) holds for all  $Ge_{15}Te_{85}$  glasses by measuring their excess heat capacity  $C_p^{\rm exc}(T)$ . The excess heat capacity is the heat capacity of the crystal  $C_p^{\rm x}(T)$  curve over that of the glass or the liquid  $C_p^{\rm g,l}(T)$ ,  $C_p^{\rm exc}(T) = C_p^{\rm g,l}(T) - C_p^{\rm x}(T)$ , which can be obtained from (crystal) rescan-subtracted DSC curves. It therefore constitutes the configurational component of the heat capacity by assuming that the vibrational components of the glass and crystals are equal [16, 17]. As shown in Figure 1a, upon reheating at a constant heating rate of  $\theta_h^{\rm s} = 20$  K/min, the  $C_p^{\rm exc}(T)$  curves of the MQ and ASD phases show a glass transition followed by an endothermic overshoot when entering the UCL and the UCL afterwards. Since all samples feature a glass transition, MQ and ASD  $Ge_{15}Te_{85}$  are glasses at low temperatures [18]. Integrating the  $C_p^{\rm exc}(T)$ -curves and normalizing them to a point in the UCL reveals the different enthalpy states of the glasses, from which  $\Delta H_g^{\rm s}$  is obtained, as depicted in Figure 1b. The fictive temperature is found from the crossing point of linearly extrapolated glassy and UCL

enthalpies [19], as sketched in Figure 1b for the standard glass. The resulting  $\Delta H_{\rm g}^{\rm s}$  values for MQ and ASD glasses show the expected linear dependence on  $T_{\rm f}$  with a slope of  $\Delta C_{\rm p} = \Delta H_{\rm g}^{\rm s}/\Delta T_{\rm f} = 16.9 \, {\rm J \ mol^{-1} \ K^{-1}}$  (inset of Figure 1b), demonstrating that Eq.(2) holds. As can be seen from the inset in Figure 1b,  $\Delta H_{\rm g}^{\rm s}$  changes from 660 J/mol for the least stable glass, produced upon sputtering at a voltage of 257 V, to -80 J/mol for the most stable glass, prepared upon melt-quenching with a rate of 3 K/min. The total difference in  $\Delta H_{\rm g}^{\rm s}$  hence amounts to 740 J/mol (7,6 meV/atom).

Since here ASD glasses possess higher enthalpies and fictive temperatures than the MQ states, they are considered to be less stable against relaxation [4, 20, 21]. As a result, ASD glasses exhibit an exothermic enthalpy release prior to the glass transition which is commonly observed in hyperquenched glasses reheated at a much smaller rate than the initial cooling rate [22]. Hence, the presence of this exothermic signature in  $Ge_{15}Te_{85}$  films is indicative of a high fictive temperature and a high effective cooling rate  $\theta_c^e$  which can be attributed to the sputtering process. Interestingly, this exothermic heat release and thus  $\theta_c^e$  depend on the sputtering voltage  $U_d$ . To find  $\theta_c^e$  for ASD glasses from the measured  $T_f$  values (Eq.(3)), the fragility m of the material is required. The fragility can be determined calorimetrically noting that the apparent glass transition temperature  $T_g$  is equal to the fictive temperature  $T_f$  when the subsequent heating rate  $\theta_h$  is equal to the initial cooling rate  $\theta_c$  upon vitrification [13, 23]. In this case and after rewriting Eq.(3), the fragility m can be found from [13, 14]

$$\log_{10}\left(\frac{\vartheta}{\vartheta_{\rm s}}\right) = m \cdot \left(1 - \frac{T_{\rm f}^{\rm s}}{T_{\rm f}}\right),\tag{4}$$

where  $\theta = \theta_c = \theta_h$  and thus  $T_f = T_g(\theta)$ . Note that for non-ideally strong systems like  $Ge_{15}Te_{85}$ , Eq.(4) is only strictly valid for a range of  $T_f$  values near  $T_f^s$  and hence cooling rates  $\theta$  near the standard value of  $\theta^{s} = 20$  K/min. This is because m represents the slope of the viscosity-temperature dependence at  $T_g^s = T_f^s$ . However, in systems that exhibit non-Arrhenius behavior, this slope decreases notably at temperature much higher than  $T_g^s$ . Nevertheless, Eq.(4) is valid for heating rates accessible with conventional DSC, here 3-40 K/min [2]. Fitting Eq.(4) to  $T_{\rm f}$  data obtained by DSC yields m = 55 as represented by the grey dashed line in Figure 2. Note, that the DSC and FDSC data on  $T_f(9)$  given in Figure 2 were obtained from the glass transition temperature where the reheating rate  $\theta_h$  is equal to the initial cooling rate  $\theta_h$ . In addition to conventional DSC, Flash DSC (FDSC) allows for cooling and heating rates of up to 4,000 K/s. Since the expected temperature gradient in the sample exceeds 5 °C above 700 K/s (see Supplementary Information (SI)), only  $T_{\rm f}$  data up to that rate are considered. Now in Figure 2, the combined DSC (circles) and FDSC (diamonds)  $T_{\rm f}$ data show a curvature. This is indeed expected from the intermediate fragility of  $Ge_{15}Te_{85}$ . Consequently with increasing  $\theta$ , Eq.(4) underestimates the increase in  $T_f(\theta)$ and thus fails to describe the experimental data. This deviation becomes significant at heating rates exceeding  $\sim 50$  K/s [2]. Therefore, Eq.(4) is extended to account for the non-Arrhenius behavior of non-ideal strong systems (fragility) based on the Vogel-Fulcher-Tammann (VFT) model of viscosity  $\eta(T)$  as proposed in Ref. [24]. This extension of Eq.(4) can be given by (see SI)

$$\log_{10}\left(\frac{\vartheta}{\vartheta_{s}}\right) = \log_{10}\left(\frac{\eta_{s}}{\eta(T_{f})}\right),\tag{5}$$

where  $\eta_s$  is the viscosity at the standard glass transition temperature  $T_g^s$ . Fitting Eq.(5) to all measured (F)DSC  $T_f(\theta)$  data yields a fragility of 58 (Figure 2, black dashed line) which agrees with the value obtained from low- $\theta$  Eq.(4) fitting and literature [13]. As an additional result from Eq.(5) fitting, viscosity values for  $T = T_f$  are also derived (see SI). Contrary to Eq.(4), Eq.(5) does not deviate from the experimental data with increasing  $\theta$  but instead reproduces the data and its curvature well. Therefore, Eq.(5) is now applied to the  $T_f$  values of the ASD phases obtained from Figure 1 to calculate the effective cooling rate  $\theta_c^e$  (Figure 2). It is observed that  $\theta_c^e$  shows a clear dependency on the sputtering voltage  $U_d$ : The lower  $U_d$ , the higher  $\theta_c^e$  ranging from 1,000 K/min ( $\approx$  17 K/s) at 367 V and up to 200,000 K/min ( $\approx$  3400 K/s) at 257 V. Hence, the logarithmic effective cooling rate appears to vary linearly with sputtering voltage as shown on Figure 3. Following the indicated trend,  $\theta_c^e$  would equal the standard cooling rate  $\theta_c^s$  at about 470 V. Since the fictive temperature  $T_f$  depends on  $\theta_c^e$ ,  $T_f$  depends on the sputtering voltage  $U_d$  as well. This means that by increasing the sputtering voltage, the enthalpy state of the prepared glass is also lowered.

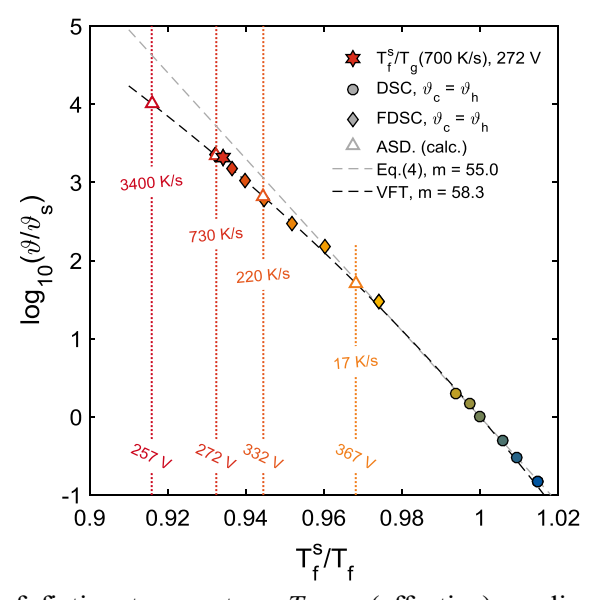


Figure 2: Dependence of fictive temperature  $T_{\rm f}$  on (effective) cooling rate  $\vartheta_{\rm c}$ . Axes are scaled according to Equation (4). Additionally to the accessible cooling and heating rates in conventional DSC, measurements are extended to the rates accessible in FDSC. Here  $\vartheta = \vartheta_{\rm c} = \vartheta_{\rm h}$ , and thus the measured glass transition temperature  $T_{\rm g}$  during the upscan is equal to the fictive temperature  $T_{\rm f}$  of this glassy state. Heating the ASD glass prepared at 272 V at its calculated cooling rate of ~700 K/s yields  $T_{\rm g} \approx T_{\rm f}$  (red star) and thereby verifying this argument. Equation (4) is fitted conventional DSC data (circles) and yields a fragility of 55 (dashed grey line). DSC and FDSC (diamonds) data is fitted by Equation (5), which is able to describe both, the low and high rate data points, whereby a fragility of 58 is found (dashed black line). Since the fitted Equation (5) describes the experimental data well, this formula is used to calculate the effective cooling rate  $\vartheta_{\rm c}^{\rm c}$  for the ASD glassy phases from the  $T_{\rm f}$  values (dotted lines) obtained from Figure 1b (open triangles). Sputtering voltages  $U_{\rm d}$  and calculated  $\vartheta_{\rm c}^{\rm c}$  values for ASD Ge<sub>15</sub>Te<sub>85</sub> are given in the figure.

As stated earlier, when  $\theta_c = \theta_h$ , the measured glass transition temperature is equal to  $T_f$ . Therefore, when an ASD glass is reheated at  $\theta_c^e$ , the measured glass transition temperature  $T_g$  should be equal to  $T_f$ . To test this hypothesis, the ASD glass

prepared at 272 V is heated at 700 K/s which is almost equal to its calculated  $\theta_c^e$ . As shown in Figure 2, the measured  $T_g$  at that rate (red star) agrees well with the fictive temperature of that ASD glass ( $C_p^{exc}$  curve given in the SI). This result shows that calculating the effective cooling rate  $\theta_c^e$  from Eq.(5) yields reliable results for ASD glasses that were prepared not by rapid cooling but by PVD.

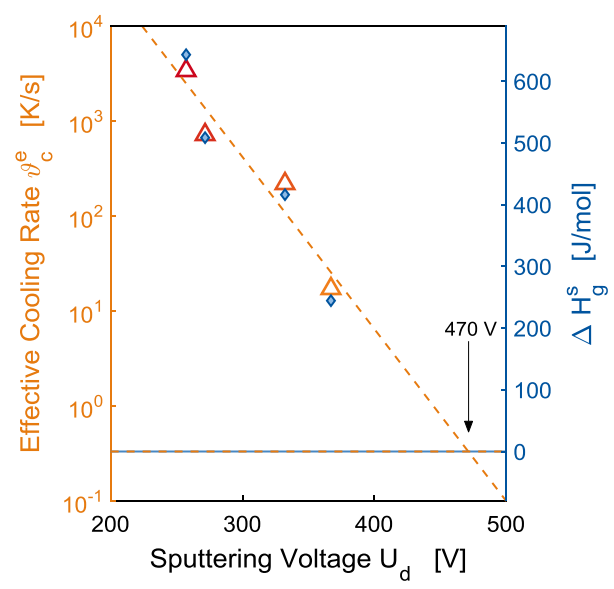


Figure 3: Calculated effective cooling rate  $\theta_c^e$  and enthalpy state  $\Delta H_g^s$  as a function of sputtering voltage  $U_d$ . According to this extrapolation, a standard glass on an unheated substrate would be obtained at a sputtering voltage of 470 V. Furthermore, a more stable glass could be obtained at higher sputtering voltages.

Our study reveals that the effective cooling rate  $\theta_c^e$  of ASD glasses lays in the region of  $\sim 10^3$  K/s. Another study suggests a value of  $\sim 10^4$  K/s for the prominent PCM  $\rm Ge_2Sb_2Te_5$  in its glassy ASD phase [25]. Both are far below the rate necessary for melt-quenching from above the melting temperature  $T_{\rm m}$  of a PCM of  $\sim 10^9$  K/s [9]. This means that  $\theta_e^c$  of usual ASD glasses is about five orders of magnitude lower. Therefore, glassy PCMs obtained by melt-quenching from above  $T_{\rm m}$  should thus be less stable than ASD glasses prepared by PVD. As a consequence, this should result in a higher crystal growth velocity in MQ glasses of PCMs, which explains the observation reported earlier for AIST [9].

The ability to tune the effective cooling rate  $\theta_c^e$  and thus the fictive temperature  $T_f$  of the resulting glasses by controlling the sputtering voltage  $U_d$  during sputter deposition provides a novel means of adjusting the enthalpy level of the resulting asdeposited glassy phase. This finding could be exploited to help prepare ultra-stable glasses (USGs). It has been shown that USGs, i.e. glasses in a particularly low enthalpy state, can be synthesized by increasing the substrate temperature to around  $T/T_g = 0.85$  during the deposition process [21]. Our study reveals an additional parameter for tuning the enthalpy state namely the sputtering voltage  $U_d$ . As reported here, a higher  $U_d$  lowers the enthalpy state of the resulting glass. A combined approach of adjusting both, the substrate temperature and the sputtering voltage may yield

glassy states even lower in enthalpy. It has been suggested that USGs can form on heated substrates due to the increased mobility of constituent particles on the film surface. The added mobility enables each particle to explore a greater fraction of the energy landscape and reach a lower minimum. Extending on this interpretation it can be hypothesized that the increased kinetic energy of the particles at the surface of the film deposited at a higher voltage allows for additional exploration of the energy landscape in order to access the lowest minima and thus lower enthalpy states.

On the other hand, when rapidly quenched material is required, as for calorimetric measurements, to mimic the fast switched glassy phase of e.g. PCM memory devices, a low substrate temperature in combination with a low sputtering voltage should yield the highest enthalpy states of the resulting glass and thus should result in an *ultra-unstable* glass. This might enable bypassing the experimentally challenging task to vitrify large amounts of highly fragile and rapid crystallizing glass formers at highest cooling rates during melt-quenching. It also helps engineer the enthalpy level of the glassy state by adjusting the sputtering voltage and the substrate temperature.

## Acknowledgements

The authors acknowledge funding from the Deutsche Forschungsgemeinschaft (DFG) via the collaborative research center Nanoswitches (SFB 917). PL acknowledge funding from NSF-DMR grant#: 1832817.

## **Methods**

Powders of  $Ge_{15}Te_{85}$  were prepared at different sputtering voltages at a base pressure of  $3\times10^{-6}$  mbar by magnetron sputter deposition from a stoichiometry target. An overview of the parameters of the sputter deposition process are given in the Supplementary Information (SI) The material was deposited onto thin metal sheets and peeled off upon bending of the sheets. Film thickness as well as the measured composition by EDX are given in the SI. Between the measurements, samples were stored in a deep-freezer at -30 °C in order to prevent the samples from aging and structural relaxation.

DSC measurements were performed in a PerkinElmer Diamond DSC and FDSC measurements in a Mettler-Toledo Flash DSC 1. The measured temperature of both DSC and FDSC data was calibrated by the melting onset of indium at the utilized heating rate as discussed in the SI.

## References

- [1] C.T. Moynihan, Phenomenology of the Structural Relaxation Process and the Glass Transition, in: R. Seyler (Ed.) Issignment of the Glass Transition, ASTM International, West Conshohocken, 1994, pp. 32-49.
- [2] G.W. Scherer, Relaxation in Glass and Composites, Wiley, New York, 1986.
- [3] C.A. Angell, K.L. Ngai, G.B. McKenna, P.F. McMillan, S.W. Martin, Journal of Applied Physics, 88 (2000) 3113-3157.
- [4] S.F. Swallen, K.L. Kearns, M.K. Mapes, Y.S. Kim, R.J. McMahon, M.D. Ediger, T. Wu, L. Yu, S. Satija, Science, 315 (2007) 353-356.
- [5] I. Lyubimov, M.D. Ediger, J.J. de Pablo, J Chem Phys, 139 (2013) 144505.
- [6] C.A. Angell, Science, 267 (1995) 1924-1935.
- [7] J. Akola, J. Larrucea, R.O. Jones, Physical Review B, 83 (2011).
- [8] J.Y. Raty, W. Zhang, J. Luckas, C. Chen, R. Mazzarello, C. Bichara, M. Wuttig, Nature Communications, 6 (2015) 7467.
- [9] M. Salinga, E. Carria, A. Kaldenbach, M. Bornhofft, J. Benke, J. Mayer, M. Wuttig, Nat Commun, 4 (2013) 2371.
- [10] P.G. Debenedetti, F.H. Stillinger, Nature, 410 (2001) 259.
- [11] C.T. Moynihan, A.J. Easteal, M.A. Bolt, J. Tucker, Journal of the American Ceramic Society, 59 (1976) 12-16.
- [12] J.A. Kalb, M. Wuttig, F. Spaepen, Journal of Materials Research, 22 (2007) 748-754.
- [13] S. Wei, P. Lucas, C.A. Angell, Journal of Applied Physics, 118 (2015) 034903.
- [14] L.M. Wang, V. Velikov, C.A. Angell, J Chem Phys, 117 (2002) 10184-10192.
- [15] R. Böhmer, K.L. Ngai, C.A. Angell, D.J. Plazek, J Chem Phys, 99 (1993) 4201-4209.
- [16] C.A. Angell, S. Borick, Journal of Non-Crystalline Solids, 307-310 (2002) 393-406.
- [17] H.L. Smith, C.W. Li, A. Hoff, G.R. Garrett, D.S. Kim, F.C. Yang, M.S. Lucas, T. Swan-Wood, J.Y.Y. Lin, M.B. Stone, D.L. Abernathy, M.D. Demetriou, B. Fultz, Nature Physics, 13 (2017) 900-905.
- [18] E.D. Zanotto, J.C. Mauro, Journal of Non-Crystalline Solids, 471 (2017) 490-495.
- [19] C.T. Moynihan, A.J. Easteal, J. Wilder, J. Tucker, J. Phys. Chem., 78 (1974) 2673-2677.
- [20] C.T. Moynihan, S.N. Crichton, S.M. Opalka, Journal of Non-Crystalline Solids, 131-133 (1991) 420-434.
- [21] H.B. Yu, M. Tylinski, A. Guiseppi-Elie, M.D. Ediger, R. Richert, Physical Review Letters, 115 (2015) 185501.
- [22] V. Velikov, S. Borick, C.A. Angell, The Journal of Physical Chemistry B, 106 (2002) 1069-1080.
- [23] C.A. Angell, Chem Rev, 102 (2002) 2627-2650.
- [24] C.A. Angell, L.-M. Wang, Biophysical Chemistry, 105 (2003) 621-637.
- [25] J. Pries, S. Wei, M. Wuttig, P. Lucas, Advanced Materials, 31 (2019) 1900784.